Eur. Phys. J. D **34**, 119–124 (2005)
DOI: 10.1140/epjd/e2005-00131-8

THE EUROPEAN
PHYSICAL JOURNAL D

Low temperature and low pressure CO oxidation on gold clusters supported on MgO(100)

O. Meerson, G. Sitja, and C.R. Henry[a]

CRMCN[b]-CNRS, Campus de Luminy, Case 913, 13288 Marseille Cedex 09, France

Received 6 September 2004

Abstract. CO oxidation has been investigated on Au/MgO(100) model catalysts at RT and low pressure. The gold particles prepared by UHV evaporation on clean MgO surfaces are characterized by HRTEM. The gold particles are FCC single crystals or multiple twins with five-fold symmetry. Infrared spectroscopy indicates that two types of adsorption sites are present which correspond to loosely and strongly bound CO. The equilibrium CO coverage for the strongly bound CO is smaller than 0.1 ML. CO titration experiments show that oxygen does not dissociate on the gold nanoparticles. The CO oxidation reaction is studied at RT by molecular beam methods. A steady state CO reaction probability up to 0.50 is measured, for the first time at low pressure, for gold particles with a mean size of 1.5 nm. A reaction mechanism is proposed in which CO adsorbed on low coordinated gold atoms reacts with oxygen adsorbed molecularly, possibly at the Au/MgO interface.

PACS. 61.46.+w Nanoscale materials: clusters, nanoparticles, nanotubes, and nanocrystals – 34.50.Lf Chemical reactions, energy disposal, and angular distribution, as studied by atomic and molecular beams

1 Introduction

Gold is essentially used for its chemical inertness, which is explained, by the very low adsorption energy and high dissociation barriers for gases [1]. In the last years since the work of Haruta which clearly established that tiny gold clusters supported on oxides are very active for CO oxidation at RT [2], a huge quantity of papers has appeared to try to understand this unexpected fact (see the following excellent reviews on the subject [3–5]). In fact, already in the early seventieth, several papers dealing with the catalytic properties of gold clusters appeared but nobody paid attention, at this time [6]. The reactivity of free Au ions towards D_2 has been studied for the first time by Cox et al. [7], which showed that cations are active while only anions with an even number of atoms react with oxygen. Finally, Whetten and co-workers evidenced that gold ions can make the CO oxidation [8] and the first true turnover was evidenced in the group of Wöste [9]. Size selected Au clusters (1–20 atoms) have been soft-landed on MgO thin films by Heiz et al. They have shown that only 8 atoms (or larger) gold clusters were active for CO oxidation [10]. Calculation showed that the different energetic barriers for the reaction where notably reduced if the 8-atoms gold cluster was sited on an oxygen vacancy on the MgO substrate that resulted on a partial charge transfer from the substrate to the gold clusters [10]. In that case, molecular oxygen reacted with adsorbed CO. Recent ab initio calculations by Molina and Hammer have shown that neutral gold clusters supported on MgO(100) surfaces can catalyse the CO oxidation [11]. Haruta and coworkers have shown that 1 nm Au clusters supported on a fully hydroxylated MgO powders were very active towards CO oxidation [12]. All the experiments that have shown a true turnover for CO oxidation on supported gold have been performed at relatively high pressure (several mbar). Attempts to observe CO oxidation under UHV environment on Au/TiO_2 (110) failed although atomic oxygen was shown to be very reactive in these conditions [13]. It was believed that the rate-limiting step was the oxygen dissociation on the gold clusters. Other remaining open questions on gold catalysis concern the oxidation state of the gold clusters, the role of the interface, the structure of the active gold particles and their optimum size.

In this study we have tried to minimize the unknown experimental parameters in order to answer to some of the open questions concerning the intriguing reactivity of small supported gold clusters. Gold clusters where grown by atomic deposition under UHV on cleaved MgO(100) surfaces expecting to get clean metallic clusters in epitaxy on the substrate [14,15]. The adsorption of CO was studied by molecular beams method [16] and infrared spectroscopy [17] and the CO oxidation was investigated at

---

[a] e-mail: `henry@crmcn.univ-mrs.fr`

[b] CRMCN is associated to Universities of Aix-Marseille 2 and 3.

low pressure by molecular beam methods allowing a direct measurement of the reaction probability [16].

2 Experimental

The MgO(100) surfaces have been cleaved under UHV [18] or in air in order to increase the density of defects, then the density of clusters [19]. In the later case the MgO surface was cleaned by heating under UHV at 700 °C during five hours in order to get a clean surface [20]. The cleanness of the substrate was checked in situ by an Auger spectrometer. The gold deposition was performed under UHV using a Knudsen cell giving a reproducible flux of gold atoms. During the deposition the sample was kept at RT or at 200 °C. The gold deposit was characterised in situ by AES. At the end of the reactivity measurements the sample was covered by a thin carbon layer, which was subsequently stripped off in a 10% aqueous solution of hydrochloric acid. The carbon layer containing the gold clusters was observed by TEM after mounting on a copper TEM grid. Conventional TEM observations were made with a Jeol 2000 FX microscope operated at 200 kV. HRTEM observations were performed at the Fritz Haber Institute in Berlin with a Phillips CM 200 HRTEM equipped with a Field Emission Gun and operated at 200 kV. The reactivity measurements were performed in situ using molecular beam methods (see the detail of the experimental set-up in Ref. [16]). A molecular beam of CO was generated by supersonic expansion; the beam is modulated by a movable shutter operated by a stepped motor. Oxygen was introduced isotropically by a leak valve. The unreacted molecules and reaction products were detected by a differentially pumped quadrupole mass spectrometer synchronised to the beam shutter. Infrared experiments were performed in another experimental system previously described [17]. The measurements were made in transmission mode using a Mattson 6202 FTIR spectrometer at a resolution of 8 cm^{-1}. The IR spectra were recorded when the equilibrium coverage was reached, at a given temperature and a given CO pressure.

3 Growth and structure of the gold clusters

The gold clusters have been grown under UHV (pressure smaller or equal to 1×10^{-9} mb during deposition) on clean MgO surfaces kept at RT or 200 °C. Figure 1 shows a typical TEM picture and a size histogram corresponding to a deposit at 200 °C on an air cleaved substrate. The clusters have a mean size of 5 nm and a number density of 1.6×10^{12} clusters per cm^2. On the Auger spectra the Au and O lines from the substrate are clearly seen confirming the Volmer-Weber growth mode [15,19]. The sample was kept at 200 °C and the intensity of the Auger peak was measured. Annealing at 200 °C during several days revealed that the deposit was not stable. Indeed, the intensity of the gold Auger peak decreased while no new peaks (e.g. carbon) was detected. We explained this decay by a slow sintering of the particles.

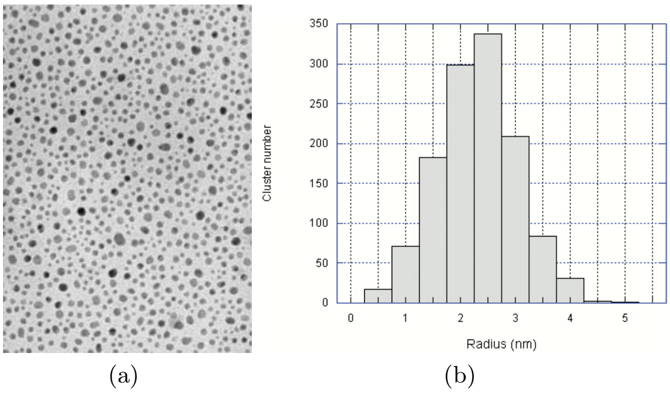

(a) (b)

Fig. 1. Au clusters grown at 200 °C on an air-cleaved MgO(100) surfaces. (a) TEM picture, (b) size distribution.

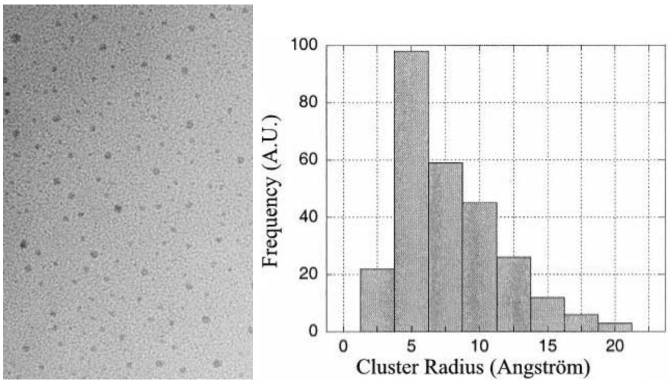

(a) (b)

Fig. 2. Au clusters grown at RT on a UHV-cleaved MgO(100) surface. (a) TEM picture, (b) size distribution.

Figure 2 presents a TEM picture and a the size histogram from a RT deposit on a UHV cleaved substrate. The mean diameter of the gold clusters is 1.5 nm and their density is 1.9×10^{12}/cm^2. However the size distribution is asymmetric that probably means that some particles are not visible by TEM (the limit of detection is around 0.5 nm). This is supported by a previous study of the nucleation of gold on MgO(100) showing that the density of clusters depends on the substrate temperature in following an Arrhenius law [19]. Extrapolating the saturation density to RT one gets 1×10^{13} clusters/cm^2, which is much larger than the value measured here by TEM. However the nucleation study was made on MgO substrates cleaved under nitrogen then we expect a slightly lower density on a UHV cleaved substrate [20]. Auger spectroscopy has shown that such deposits were stable at RT during several hours but after 2 days a significant decrease of the Au peaks and simultaneous increase of the O peaks suggested that even at RT a slow coalescence process was occurring. Figure 3 displays HRTEM pictures obtained on the deposit corresponding to Figure 2. Systematic investigation on several images has shown that three types of particles are observed: square particles exhibiting (200) fringes (Fig. 3a), triangular particles with (220) fringes (Fig. 3b) and multiply twinned particles (MTP) with decahedron or

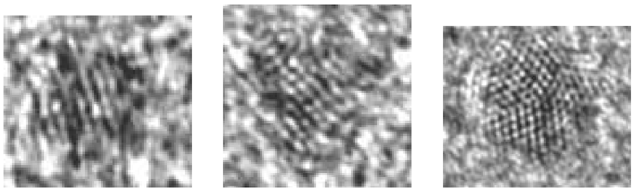

(a) (b) (c)

Fig. 3. HRTEM pictures of gold clusters corresponding to Figure 2. (a) Square particle (100) oriented exhibiting {200} lattice fringes. (b) Triangular particle (111) oriented exhibiting {220} lattice fringes. (c) Multiply-twinned particle: decahedron.

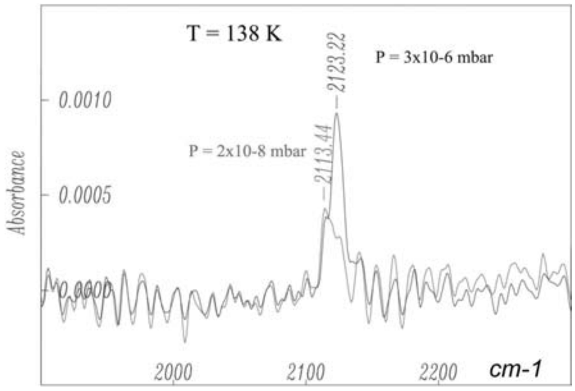

Fig. 4. Infrared spectra recorded at 138 K, under a CO background pressure of 2×10^{-8} mb (clear spectrum) and 3×10^{-6} mb (dark spectrum), on 6 nm gold particles grown on MgO(100).

icosahedron shapes (Fig. 3c). The square particles grow with a (100) plane parallel to the substrate; they have probably the shape of a truncated pyramid [15]. The triangular particles grow with a (111) plane parallel to the MgO substrate and they are probably the shape of a tetrahedron. These findings are compatible with (100) and the (111) epitaxies observed for gold on MgO at high temperature [15] but here (at RT) we cannot tell that the particles are in epitaxy because the gold clusters are azimuthally disoriented. Moreover the MTP represent a large fraction of the particles observed with lattice resolution. However, as many gold clusters cannot be observed at high resolution (due to a too small size or a bad orientation relatively to the electron beam) it is not possible to tell what is the fraction of the total gold clusters that present five-fold symmetry. Occasionally some large particles (≈7 nm) are observed, they are (100) oriented and probably results from coalescence of smaller clusters.

4 Reactivity measurements

4.1 CO adsorption

Figure 4 presents IR spectra of CO adsorbed at 138 K at two different equilibrium coverages on gold particles (6 nm) on MgO(100). At low coverage we see a peak with a maximum at 2113 cm^{-1}. At high coverage (close to saturation) the peak appears at 2123 cm^{-1}. However as a shoulder at 2113 cm^{-1} is still present, we conclude that two adsorption sites are present, otherwise we would expected a single peak shifting with coverage in the case of a unique adsorption sites. The adsorption of CO has been studied at RT using the pulsed molecular beam method [16]. Figure 5 displays adsorption-desorption pulses of CO at RT for gold particles of 6 nm. Only a small proportion of the desorbed signal show a measurable relaxation type of about 0.8 s. It corresponds to a maximum value for the equilibrium coverage of 0.1 ML. Assuming a frequency factor of 1×10^{13} Hz the maximum value of the adsorption energy would be 17 kcal/mol.

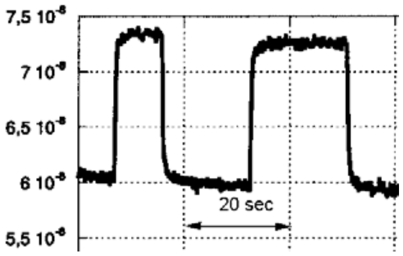

Fig. 5. RT adsorption-desorption pulses of CO from gold nanoparticles of 1.5 nm on MgO(100).

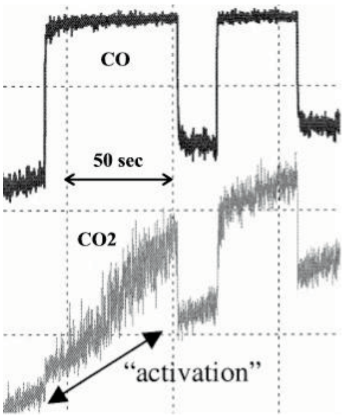

Fig. 6. RT CO oxidation on 1.5 nm gold clusters on MgO(100). CO and CO_2 pulses desorbing from the sample are displayed at the same scale. An activation period is seen on the first CO_2 pulse. The CO equivalent pressure (CO beam) was 5×10^{-8} mb and the isotropic O_2 pressure was 1×10^{-8} mb.

4.2 CO oxidation

For the reaction, the UHV chamber is filled with an isotropic pressure of oxygen and pulses of CO (the equivalent pressure in the beam was 5×10^{-8} mb) are directed to the sample surface (the size of the beam is smaller than the size of the sample). The CO and CO_2 desorbing from the sample are simultaneously recorded by the mass spectrometer. The sample with particles having a mean size of 1.5 nm (see Figs. 2 and 3) has shown a very high activity. However at the beginning of the CO pulse the CO_2 signal was weak and after about 30 s it increased rapidly (see Fig. 6) and after several minutes it reached a steady state (see Fig. 7). At steady state the reaction probability is about 0.5 (it could be even larger if some CO is directly reflected from the MgO substrate). On larger clusters only a weak activity has been measured. At RT for 4 nm gold particles the reaction probability is 0.05. When the oxygen pressure increased the reaction probability decreased.

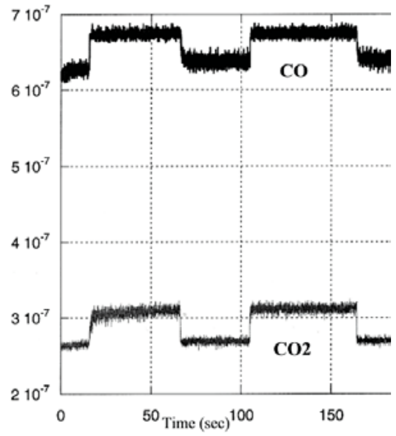

Fig. 7. Steady state CO oxidation on 1.5 nm gold clusters on MgO(100) at RT. The CO and CO_2 pulses desorbing from the sample are displayed at the same scale. The CO equivalent pressure (CO beam) was 5×10^{-8} mb and the isotropic O_2 pressure was 1×10^{-8} mb.

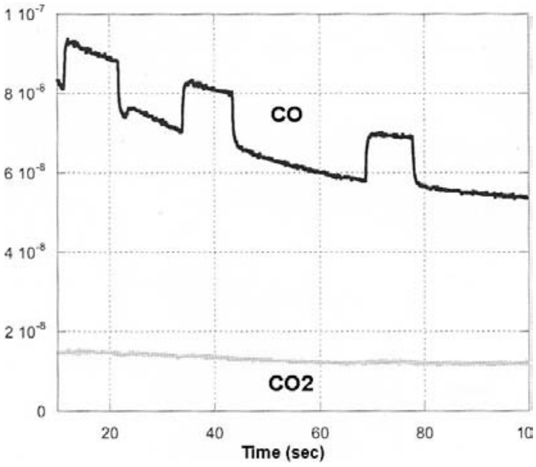

Fig. 8. CO titration experiment showing that no dissociated oxygen was adsorbed on the Au/MgO(100) sample after exposure to 600 L of molecular oxygen. The CO and CO_2 signals desorbing from the sample are displayed at the same scale.

In order to check if CO reacts with atomic or molecular oxygen we have performed the following experiment. The 1.5 nm gold particles were exposed to 600 L of molecular oxygen, and then after pumping the oxygen in the chamber the sample was exposed to a series of CO pulses. As it can bee seen in Figure 8, no CO_2 was produced. If oxygen was dissociated it would has stuck on the gold particles [13] and readily reacted with CO pulses. Conversely, if oxygen was adsorbed molecularly it would have desorbed during pumping of the oxygen then no oxygen would be left on the clusters. Therefore we conclude from this experiment that oxygen does not dissociate on the gold before to react with adsorbed CO.

5 Discussion

5.1 Structure of active gold clusters

For gold/TiO_2 catalysts prepared by chemical methods the structure of the gold particles has been investigated by HRTEM. Haruta and coworkers [21] have found that the gold particles have a hemispherical shape with an FCC structure and that they are in the (111) orientation on anatase TiO_2 (112) facets. In another study we have shown that, for the same system (prepared by deposition-precipitation), the particles had the shape of truncated octahedra with re-entrant part and that the particles with smooth facets were less active than those with rough facets [22]. In the case of UHV deposition of atoms, Au particles grow at high temperature (higher than 200 °C) with a truncated octahedron shape (equilibrium shape) [14,15,23]. Here we observed that we loose epitaxy at RT and also that a large number of MTP with five fold symmetry appear. Fivefold symmetry is common on free gold particles, and on supported particles when the metal-support interaction is weak [24]. On Au/MgO (hydroxylated) catalysts prepared by deposition-precipitation, particles of mean size of 1 nm and icosahedral structure were observed by Debye Functional Analysis (an X-ray diffraction technique allowing to analyse the structure of very small clusters) [12]. In the present study on a clean MgO(100) surface we have found, for RT growth, both FCC particles with a truncated octahedron shape and MTP particles with fivefold symmetry however it is not possible to tell if all the particles are active for the CO oxidation.

5.2 CO adsorption

We observed that part of gold surface atoms (less than 10%) bind CO rather strongly (up to 17 kcal mole). On extended Au surfaces an isosteric heat of adsorption of 12 to 14 kcal/mol has been measured [25–27]. The higher adsorption energy is probably due to low coordinated sites (edges and possibly defects) in agreement with theoretical calculations [11]. On Au extended surfaces the CO stretch frequency is found between 2108 and 2113 cm^{-1} at high coverage [25]. On small Au clusters supported on an FeO(111) thin film the CO stretch frequency at saturation decreases from 2132 cm^{-1} to 2108 cm^{-1} as cluster size increases [28]. On the contrary on Au/γ-Al_2O_3 single crystals the CO stretch frequency increases with clusters size from 2100 to 2110 cm^{-1} [29]. In the present measurements we observe a first band 2113 cm^{-1} and a second one 2123 cm^{-1} appears by increasing CO pressure (i.e. higher coverage). They correspond to two different sites because the shift due to coverage increase for extended surfaces is in the opposite direction [25,26]. It is clear that the first populated sites (2113 cm^{-1}) correspond to stronger CO bonding which are tentatively attributed to low coordinated sites (like edges) and the second band at 2123 cm^{-1} to CO adsorbed on smooth facets. This assignment is in line with Au/γ-Al_2O_3 [29] but not with

Au/FeO [28]. This difference is possibly due to a support effect.

5.3 Oxygen adsorption

Long-time ago it has been shown that in the oxygen pressure range 10^{-6} to 10^{-3} mb no oxygen can adsorb at RT on bulk (polycrystalline) gold, while atomic oxygen readily adsorbs at RT and desorbs at 654 K [30] in agreement with ab initio calculations [31]. On gold (110) molecular oxygen does not adsorb between 300 and 500 K up to a pressure of 1.4 bar [32]. However, on small (2–22 atoms) free clusters it has been shown that oxygen adsorbs molecularly [7]. On Au nanoparticles grown under UHV on $TiO_2(110)$ molecular oxygen even at 250 mb was not observed to dissociate, while atomic oxygen is readily adsorbed as seen by TPD [13]. In fact these experiments show clearly that molecular oxygen does not dissociate even on Au clusters in the size range where they are active in catalysis but they do not prove that molecular oxygen is not adsorbed (at least physisorbed) on the gold particles because during the time between oxygen exposure, pumping down and either TPD or CO dosing the adsorbed oxygen molecules are desorbed. In our experiments after a very large exposure to molecular oxygen (600 L) no chemisorbed (atomic) oxygen is observed by CO titration. The time between the end of oxygen exposure and CO titration is about 100 s which is smaller than the expected residence time (around 5000 s) of atomic oxygen taking a desorption energy of 100 kJ/mol and a pre-exponential factor of 5.5×10^{12} Hz [13]. Conversely we can conclude that if molecular oxygen was adsorbed during oxygen exposure its desorption energy is smaller than 80 kJ/mol (assuming that adsorbed molecular oxygen reacts with CO).

5.4 Reaction mechanism

Two mechanisms based on the Langmuir-Hinshelwood frame have been proposed for the CO oxidation on supported gold nanoparticles: molecular adsorption of both reactants and formation of CO_2 via a carbonate intermediate species [4,10,11] or reaction of adsorbed molecular CO with dissociatively adsorbed oxygen [13,33] (as in the case of the Pt metal). The first mechanism is supported by experiments on gas phase clusters showing clearly the presence of both CO and molecular oxygen on the clusters, however in that case the clusters are ionised. It is eventually possible that both mechanisms take place as suggested from calculations [34] and recent experiments [35]. However in the case of Au nanoparticles supported on clean MgO one can rule out the dissociation of oxygen in agreement with the calculation of Molina and Hammer [11]. From the present results we can draw the following pictures: CO is adsorbed on low coordinated Au atoms (edges, defects), oxygen is adsorbed molecularly on some unidentified sites and they react to form CO_2. The fact that only small clusters ($\leq$1.5 nm) are active is partly explained by the necessity to have enough low coordinated sites to adsorb enough CO but it is not sufficient because otherwise open Au extended surfaces would be active. In our case it is difficult to believe that we have oxidized Au atoms (even at the interface) [3], charge transfer from oxygen vacancies [12] or that we have quantum size effect [36]. Thus the more plausible explanation (at least for the case of Au/MgO) is given by the calculations of Molina and Hammer [11]. In that case, when only one re-entrant layer is present at the interface between the MgO(100) surface and a truncated octahedron gold particle, CO is adsorbed at the edge of the second gold layer and an oxygen molecule is stabilized between gold and MgO in the re-entrant edge, then the activation barrier for reaction is considerably reduced in comparison with other sites. With this model we can understand the strong size effect because, assuming the same equilibrium shape for the gold particles on MgO [15], the situation discussed above appears only for small sizes. To verify this hypothesis it should be very important to have only one particle shape that means that we need to grow the particles at least at 200 °C to have no MTP but in that case the density of clusters would be small then the total reaction rate will be low.

6 Conclusion

In this paper we have measured for the first time a steady state reaction rate for CO oxidation on gold model catalysts at low pressure (UHV experiment). The gold catalyst were prepared by growing under UHV gold 3D nanoparticles on a UHV cleaved MgO(100) surface. The particles have a mean size around 1.5 nm, they have an FCC structure but part of them are multiple twins with fivefold symmetry. Two different types of adsorption sites for CO are evidenced on the gold particles. The coverage corresponding to the strongly bound CO is below 0.1 ML Oxygen does not dissociate on the model catalyst. A CO reaction probability up to 0.50 has been measured by molecular beam methods. The proposed reaction mechanism is adsorption of CO on edges and defects on the gold particles and reaction with molecularly adsorbed oxygen.

Klaus Weiss from the Fritz Haber Institute (Berlin) is gratefully acknowledged for his help for HRTEM observations, Hajo Freund and Ueli Heiz for fruitful discussions. Thanks to the Alexander von Humboldt foundation for financial support (C.R.H). The work has been performed in the frame of the HPRN “OXIDESURFACES” from the fifth PCRD from European Community.

References

1. B. Hammer, J.K. Norskov, Nature **376**, 238 (1995)
2. M. Haruta et al., J. Catal. **115**, 301 (1989)
3. G.C. Bond, D.T. Thompson, Gold Bull. **33**, 41 (2000)
4. M. Haruta, CATTECH **6**, 102 (2002)
5. R. Meyer et al., Gold Bull. **37**, 72 (2004)
6. D.Y. Cha, G. Parravano, J. Catal. **18**, 200 (1970)
7. D.M. Cox et al., Z. Phys. D **19**, 353 (1991)

8. B.E. Salisbury et al., Chem. Phys. **262**, 131 (2000)
9. L.D. Socaciu et al., J. Am. Chem. Soc. **125**, 10437 (2003)
10. A. Sanchez et al., J. Phys. Chem. A **103**, 9573 (1999)
11. L.M. Molina, B. Hammer, Phys. Rev. Lett. **90**, 206102 (2003)
12. D.H. Cunningham et al., J. Catal. **177**, 1 (1998)
13. V.A. Bondzie et al., Catal. Lett. **63**, 143 (1999)
14. S. Giorgio et al., Phil. Mag. A **64**, 87 (1991)
15. S. Ferrero et al., Phys. Rev. B (submitted)
16. C.R. Henry, in *The Chemical Physics of Solid Surfaces*, Surface Dynamics, edited by D.P. Woodruff (Elsevier, 2003), Vol. 11, Ch. 9, p. 247
17. C. Goyhenex et al., Surf. Sci. **352-354**, 475 (1996)
18. C. Barth, C.R. Henry, Phys. Rev. Lett. **91**, 196102 (2003)
19. K. Hoejrup-Hansen et al., Appl. Surf. Sci. **226**, 167 (2004)
20. C. Duriez et al., Surf. Sci. **230**, 123 (1990)
21. T. Akita et al., J. Electr. Microsc. **49**, 657 (2000)
22. R. Zanella et al., J. Catal. **222**, 357 (2004)
23. S. Giorgio et al., Ultramicroscopy **38**, 1 (1991)
24. L.D. Marks, D.J. Smith, J. Microsc. **130**, 249 (1983)
25. C. Ruggiero, P. Hollins, J. Chem. Soc. Fraday Trans. **92**, 4829 (1996)
26. D.C. Meier et al., J. Phys. Chem. B **107**, 12668 (2003)
27. Y. Jugnet et al., Surf. Sci. **521**, L639 (2002)
28. C. Lemire et al., Surf. Sci. **552**, 27 (2004)
29. C. Winkler et al., Langmuir **19**, 717 (2003)
30. N.D.S. Canning et al., Surf. Sci. **141**, 240 (1984)
31. Y. Xu, M. Mavrikakis, J. Phys. Chem. B **107**, 9298 (2003)
32. A.G. Sault et al., Surf. Sci. **169**, 397 (1986)
33. M.M. Schubert et al., J. Catal. **197**, 113 (2001)
34. N. Lopez, J.K. Norskov, J. Am. Chem. Soc. **124**, 11262 (2002)
35. J.D. Stiehl et al., J. Am. Chem. Soc. **126**, 13574 (2004)
36. M. Valden et al., Science **281**, 1647 (1998)